

AperTO - Archivio Istituzionale Open Access dell'Università di Torino

Center of pressure displacement due to graded controlled perturbations to the trunk in standing subjects: the force-impulse paradigm

This is the author's manuscript

Original Citation:

Availability:

This version is available <http://hdl.handle.net/2318/1843142> since 2022-02-23T21:41:30Z

Published version:

DOI:10.1007/s00421-021-04844-9

Terms of use:

Open Access

Anyone can freely access the full text of works made available as "Open Access". Works made available under a Creative Commons license can be used according to the terms and conditions of said license. Use of all other works requires consent of the right holder (author or publisher) if not exempted from copyright protection by the applicable law.

(Article begins on next page)

1 *Original Article*

2 **Center of pressure displacement due to graded controlled**
3 **perturbations to the trunk in standing subjects: the force-**
4 **impulse paradigm**

5 Maria Paterna¹, Zeevi Dvir², Carlo De Benedictis¹, Daniela Maffiodo¹, Walter Franco¹,
6 Carlo Ferraresi¹, Silvestro Roatta^{3*}

7

8 ¹ Dept. of Mechanical and Aerospace Engineering, Politecnico di Torino, Torino, Italy

9 ² Dept. of Physical Therapy, Faculty of Medicine, Tel Aviv University, Tel Aviv, Israel

10 ³ Dept. of Neuroscience, University of Torino, Torino, Italy

11

12

13 *Correspondence to:

14 Silvestro Roatta

15 Dip. di Neuroscienze, Università di Torino

16 c.so Raffaello 30, 10125, Torino, Italy

17 tel +39 011 6708164

18 e-mail: silvestro.roatta@unito.it

19 ORCID: [0000-0001-7370-2271](https://orcid.org/0000-0001-7370-2271)

20

21

22

23

24 **ABSTRACT**

25 *Purpose:* Many studies have investigated postural reactions (PR) to body-delivered
26 perturbations. However, attention has been focused on the descriptive variables of
27 the PR rather than on the characterization of the perturbation. This study aimed to
28 test the hypothesis that the impulse rather than the force magnitude of the
29 perturbation mostly affects the PR in terms of displacement of the center of foot
30 pressure (ΔCoP).

31 *Methods:* Fourteen healthy young adults (7 males and 7 females) received two
32 series of 20 perturbations, delivered to the back in the anterior direction, at mid-
33 scapular level, while standing on a force platform. In one series, the perturbations
34 had the same force magnitude (40 N) but different impulse (range: 2-10 Ns). In the
35 other series the perturbations had the same impulse (5 Ns) but different force
36 magnitude (20-100 N). A simple model of postural control restricted to the sagittal
37 plane was also developed.

38 *Results:* The results showed that ΔCoP and impulse were highly correlated (on
39 average: $r=0.96$) while the correlation ΔCoP –force magnitude was poor ($r=0.48$)
40 and not statistically significant in most subjects. The normalized response,
41 $\Delta\text{CoP}_n=\Delta\text{CoP}/I$, was independent of the perturbation magnitude in a wide range of
42 force amplitude and impulse and exhibited good repeatability across different sets
43 of stimuli (on average: $\text{ICC}=0.88$). These results were confirmed by simulations.

44 *Conclusion:* The present findings support the concept that the magnitude of the
45 applied force alone is a poor descriptor of trunk-delivered perturbations and suggest
46 that the impulse should be considered instead.

47 **Keywords:** Postural reaction; perturbation; force; impulse; center of pressure; balance
48 control.

49

50 **1. INTRODUCTION**

51 Research on postural reactions (PR) has employed a variety of perturbation
52 techniques intended to simulate in laboratory conditions the events that challenge
53 the body equilibrium in real life. Two distinct approaches have been followed:
54 imparting the perturbation i) to the base of support by sliding or tilting the platform
55 (Schmidt et al. 2015; Grassi et al. 2017; Robbins et al. 2017) or ii) directly to the
56 upper body. These two perturbation modes elicit fundamentally different PR
57 (Bortolami et al. 2003; Colebatch et al. 2016; Chen et al. 2017) and thus are both
58 worth to be pursued. However, while the moving platform is easily described and
59 standardized in terms of extent and speed of displacement and rotation, description
60 and quantification of upper body perturbation are more difficult. Direct body
61 perturbation has been achieved in the most disparate of ways. Some devices were
62 based on imparting a pull force to the body by the sudden release of a weight
63 connected to the body via a cable (Martinelli et al. 2015; Maaswinkel et al. 2016;
64 Azzi et al. 2017) or employing electric actuators (Pidcoe and Rogers 1998;
65 Sturnieks et al. 2013; Fujimoto et al. 2015; Robert et al. 2018), which, however,
66 alter the subject's resting posture, thus potentially affecting the overall PR. Others
67 are based on the application of a push force imparted manually by pushing the
68 subject with the hands (Colebatch et al. 2016), or by releasing a pendulum which
69 hits the body at shoulder level (Kim et al. 2012), or by the action of a hand-held
70 device which records the force profile during contact with the subject (Kim et al.
71 2009; Pasman et al. 2019; Dvir et al. 2020). In most cases little attention was
72 devoted to the characterization of the perturbation and the relation between the
73 magnitude of the perturbation and the postural response, focusing instead on the

74 factors affecting CoP steadiness (Martinelli et al. 2015; Azzi et al. 2017; Grassi et
75 al. 2017) or its association with the risk of falling (Sturnieks et al. 2013; Fujimoto
76 et al. 2015). However, the precise identification of the input variable that better
77 correlates with the CoP response could facilitate the interpretation of the results and
78 the design of appropriate postural tests. Significantly, it could enhance testing of
79 patients affected with disorders in which the normal PR may be compromised
80 (Grassi et al. 2017; Colebatch and Govender 2019).

81 Although it is generally acknowledged that, within the boundaries of stability, the
82 greater the magnitude of the perturbation the greater is the PR (Diener et al. 1988;
83 Kim et al. 2009; Azzi et al. 2017; Forghani et al. 2017; Teixeira et al. 2019), very
84 few studies investigated this relation with upper body-directed perturbation. Kim et
85 al (2009) evidenced a positive correlation between the peak force of a body-directed
86 push perturbation and the displacement of the center of pressure (CoP). However,
87 by exploring specifically this facet of PR, we have recently observed that in young
88 men, the magnitude of the CoP response, in terms of its displacement, was better
89 correlated with the impulse than with the peak force of the postural perturbation
90 (Dvir et al. 2020). On one hand, it may seem obvious that the magnitude of the
91 perturbation cannot be simply characterized by the magnitude of the force but
92 should also depend on the duration of the push. On the other hand, the impulse,
93 indeed defined as the integral of force over time, has surprisingly not gained much
94 consideration in the literature, even though it corresponds to the momentum
95 transferred to the body. As such, it is directly related to the change in speed of the
96 body and thus to the energy transmitted by the perturbation.

97 The preliminary observation presented in Dvir et al.(2020) did not provide a clear-
98 cut indication with regard to the impulse vs. force paradigm, possibly because of
99 data dispersion. The postural perturbations were manually delivered, with high
100 intra- and inter- subject variability, in terms of force amplitude, duration and
101 impulse. This could have accounted for the intra-subject variability of the response
102 and the low Pearson correlation coefficient values observed in some subjects.

103 Aim of the present study is to reinvestigate the hypothesis that the CoP
104 displacement due to trunk-directed push perturbations is linearly correlated with the
105 magnitude of the impulse and not with the force magnitude, by means of a renewed
106 experimental approach and model simulations. In order to reduce the variability in
107 the magnitude of the perturbations a novel pneumo-tronic device was developed,
108 capable of imparting simultaneous force- and duration-controlled perturbations
109 (Ferraresi et al. 2020a, b; Maffiolo et al. 2020). In addition, the experimental results
110 are discussed and compared with a simulation of the CoP response based on a
111 simple single-link inverted pendulum model.

112 **2. METHODS**

113 *2.1 Experimental test*

114 2.1.1 Subjects

115 A group of 14 healthy young adults, 7 females (mean(SD) age: 22.7(1.7)years;
116 height: 1.62(0.05)m; weight: 54.0(4.2)kg; BMI: 20.7(1.5)kg/m²) and 7 males
117 (mean(SD) age: 23.1(2.7)years; height: 1.78(0.11)m; weight: 70.3(6.0)kg; BMI:
118 22.3(1.6)kg/m²), was recruited from the student population at the Politecnico di
119 Torino. Exclusion criteria included: recent lower extremity injury and/or fracture

120 (< 1 year), previous reconstructive surgery in the lower extremity and balance
121 deficits. All subjects provided written informed consent to participate in this study
122 which was approved by the institutional review board of the University of Torino
123 (Prot. n. 380583).

124 2.1.2 Task and instrumentation

125 The experimental task consisted of recovering balance following impulsive
126 perturbations applied to the trunk in the anterior direction while standing on a force
127 platform.

128 The force platform, a modified Shekel (Beit Keshet, Israel) device, was made up of
129 a still plate (52x36 cm) which was supported by 4 uniaxial load cells (TEDEA,
130 Israel, model 1042, rated capacity 100 kgf), mounted on a base plate. The
131 perturbation was applied by a pneumo-tronic perturbator designed and constructed
132 at the Dept. of Mechanical and Aerospace Engineering at the Politecnico di Torino.
133 The instrument is shown in Fig. 1A and was described in detail in another
134 publication (Ferraresi et al. 2020b). The closed-loop force feedback design, based
135 on the continuous monitoring of the perturbation force provided by a load cell
136 positioned in series with the tip of the perturbator, allows for the regulation of the
137 precise intensity and duration of the stimulus delivered to the subject, irrespective
138 of the mechanical compliance of the operator (Ferraresi et al. 2020b).

139 2.1.3 Procedure

140 During the test, the subjects stood barefoot on the force platform with the feet at
141 pelvic distance and with vision unobstructed. Subjects were asked to assume a

142 normal-relaxed stance and they were instructed to respond naturally. The feet
143 locations were traced onto the platform surface to ensure consistent initial foot
144 placement across test sessions for each participant. The operator stood behind the
145 subject holding the perturbator while the interface was maintained at a distance of
146 about 2 cm from the subject's back (Fig. 1B). Immediately before the starting of
147 the test, participants were familiarized with the procedure by receiving few
148 perturbations. The perturbations were delivered to the trunk always at inter-scapular
149 level (IS), given that, at this site, more reproducible responses could be obtained,
150 compared to lumbar level (Dvir et al. 2020).

151 The test comprised two series, with a break of 5 min in between. In one series,
152 namely the constant-force series, the perturbations had the same force magnitude
153 (40 N), but different impulse values (2 Ns; 4 Ns; 6 Ns; 10 Ns). In the other series,
154 namely the constant-impulse series, the perturbations had the same impulse (5 Ns)
155 but different force magnitude (20 N; 40 N; 60 N; 100 N). Based on our previous
156 experience, we operated in a range of values large enough to elicit a clearly
157 detectable response and small enough to exclude a step response. The values of 40
158 N and 5 Ns were arbitrarily chosen as intermediate values within that range. The
159 average force perturbation profiles, for each condition, are shown in Fig. 2.

160 In each series, the subjects received a total of 20 perturbations, 5 for each force
161 profile mentioned above. The sequences of perturbations, each one including 5
162 equal stimuli, were provided in random order. An inter-perturbation pause of at
163 least 10 s was allowed for returning to relaxed stance. The order of the 2 series was
164 randomized as well. A typical testing session lasted about 20 minutes.

165 2.1.4 Data processing

166 Data were extracted and processed with custom routines developed in
167 MATLAB_R2019b®. The force signal was acquired at 1000 Hz and digitally low-
168 pass filtered using a dual-pass 8th order Butterworth filter with a cut-off frequency
169 of 200 Hz. The actual magnitude of the perturbation was characterized in terms of:

- 170 • Force Amplitude (in N): the average force at the plateau. The start and the
171 end of the plateau were automatically detected as the time instants at which
172 the force signal crossed a threshold equal to 95% of the intended force
173 magnitude (see Fig. 3).
- 174 • Impulse (in Ns): the integral of force computed over the time interval in
175 which the force is greater than 0.5 N.

176 The ground reaction forces were acquired at 1000 Hz and were used to calculate
177 the coordinates of the CoP. Both coordinates were digitally low-pass filtered with
178 a dual-pass 8th order Butterworth filter with a cut-off frequency of 20 Hz. The
179 postural response, ΔCoP , was computed as the maximum CoP displacement,
180 observed within 2 s from the perturbation. The displacement (in cm) is calculated
181 from the average resting position, calculated over the 3 s preceding the perturbation.

182 2.1.5 Statistical Analysis

183 All statistical procedures were conducted using MATLAB_R2019b®.

184 Possible differences in impulse and force amplitude among the different
185 perturbation types were analyzed through a Friedman test with grouping factor

186 impulse and force amplitude for the constant-force and constant-impulse series,
187 respectively.

188 Pearson's correlation coefficient (r) was used to assess the relationship between
189 ΔCoP and the perturbation. The Fisher's Z transform was used to estimate an
190 average correlation coefficient over all subjects. Pearson's coefficient was also
191 calculated to evaluate the relationship between the postural response and the
192 physical characteristics of the subjects. The Friedman's test was used to determine
193 whether the impulse or force amplitude affect the CoP displacement.

194 Intraclass correlation coefficients ($\text{ICC}_{3,k}$), based on a mean rating ($k = 5$), absolute
195 agreement, 2-ways mixed effects model were derived to quantify the reliability of
196 the CoP response among different stimulus magnitudes while the coefficient of
197 variation (CoV) was used to assess the variability of the responses to the same
198 perturbation type. In order to evaluate whether general postural adjustments in
199 anticipation of back perturbations took place during the test, changes in resting CoP
200 were assessed within each session (comparing the beginning and the end of each
201 experimental session, average CoP computed 30-s intervals with no perturbations;
202 Wilcoxon Signed Rank Test) as well as within each of the 8 sequences of stimuli
203 of the same type (comparing the 3-s CoP baseline preceding the first stimulus and
204 the last one of the sequence; Wilcoxon Signed Rank Tests, with Bonferroni
205 correction).

206 Data in the text are expressed as mean \pm standard deviation.

207 *2.2 Single-link inverted pendulum models*

208 The human body orthostatic position perturbed with low entity disturbances
 209 occurring in the sagittal plane can be schematized by means of an inverse pendulum
 210 model (Winter et al. 1998). The basic scheme, implemented in MATLAB®
 211 Simulink® environment, represents the body as a rigid link having a single
 212 rotational degree of freedom (DoF) about the ankle joint (Fig. 4). For small
 213 oscillations of the body θ , the linearization of the model yields the following
 214 equations:

$$215 \quad \tau + mgd\theta - md^2 \frac{d^2\theta}{dt^2} - I \frac{d^2\theta}{dt^2} + F_e h_F = 0 \quad (1)$$

$$216 \quad CoP = \frac{-\tau - R_x h}{mg} \quad (2)$$

217 where τ is the correcting torque at the ankle, m is the body mass, g is the
 218 gravitational acceleration, d is the distance between ankle joint and the center of
 219 mass (CoM), I is the rotational inertia of the body about the CoM, h_F is the distance
 220 between ankle joint and the point of application of the perturbation force F_e , CoP is
 221 the center of pressure position, R_x is the horizontal component of the ground
 222 reaction force, h is the height of ankle joint with respect to the fixed base of support.

223 Although simplified models of balance control can focus on muscle stiffness alone
 224 as the main tool to achieve stabilization in quiet standing, it is well known that such
 225 passive behavior is generally not sufficient to ensure stability (Morasso et al. 1999),
 226 especially when significant external disturbances are considered. For this reason,
 227 the correcting torque at the ankle τ has been modeled as the sum of a passive and
 228 an active contribution. The passive contribution is related to the visco-elastic
 229 behavior of human tissues and is proportional to both the deformation θ and the rate

230 of deformation $\dot{\theta}$ of the joint (Engelhart et al. 2015), whereas the active contribution
231 depends on the neuromuscular control managed by the central nervous system and
232 can be modeled as a delayed PD (Proportional-Derivative) action (Van Der Kooij
233 et al. 2005). In particular, the output of the controller, i.e., the active torque at the
234 ankle, is aimed at minimizing the error θ , i.e., the current angular displacement from
235 the initial standing position ($\theta=0$). The information about the current angular
236 displacement is fed to the controller by noisy and delayed sensory feedback. Thus,
237 a constant transmission delay was introduced as the latency between the variation
238 of θ and the generation of the reflex active torque (Goodworth and Peterka 2018),
239 and an additive pink noise was introduced to account for the limitations of the
240 sensory system (Van Der Kooij and Peterka 2011; Boonstra et al. 2013; Goodworth
241 and Peterka 2018). Proportional and derivative gains of the PD control model then
242 need to be identified, to match the characteristics of a given subject and to achieve
243 stability. (Van Der Kooij et al. 2005; Van Der Kooij and Peterka 2011; Goodworth
244 and Peterka 2018).

245 With the limited aim of investigating the theoretical dependence of the CoP
246 response to force and impulse of the perturbation, the model was configured as
247 follows: 1) anthropometric parameters were set equal to average values computed
248 over the participants to the experimental study (with reference to Fig. 4: $m = 62$ kg,
249 $l = 1.70$ m, $h = 0.1$ m, $d = 0.6l$, $I = ml^2/12$, $h_F = 1.2$ m); 2) the coefficients of the
250 passive response were set according to the literature (Engelhart et al. 2015); 3) the
251 latency between the generation of the active torque and the variation of θ was set to
252 the constant value of 90 ms, according to the literature (Goodworth and Peterka

253 2018); 4) active control parameters and noise level were estimated by an iterative
254 least-squares fitting used to match the simulation with the average experimental
255 postural response.

256 The CoP response to a given perturbation was obtained from the average of 5
257 distinct simulations, thus accounting for the variability introduced by sensory noise.

258 **3. RESULTS**

259 *3.1 Results of the experimental trials*

260 A representative recording of a single perturbation along with the postural response
261 is shown in Fig. 3.

262 The actual magnitudes for the different experimental perturbation types are shown
263 in Fig. 5 for the two series. In the constant-force series, the perturbator delivered
264 stimuli with different impulses and with similar force amplitude values (on average,
265 39.54 ± 3.01 N) although the actual force amplitude appeared to depend on stimulus
266 type ($p < 0.01$) (Figure 5A). Similarly, the perturbation types in the constant-
267 impulse series were well characterized by distinct force values and similar impulse
268 values (on average, the impulse was equal to 4.60 ± 0.28 Ns) although a significant
269 dependence of impulse on stimulus type was observed ($p < 0.01$) (Fig. 5B).

270 Note that, while impulse was precisely controlled among subjects, peak force
271 exhibited some increased dispersion at 2 Ns compared to other impulse levels,
272 possibly due to the difficulty in controlling short-duration perturbations.

273 In all subjects, ΔCoP exhibited a significant ($p < 0.001$) and extremely good linear
274 correlation with the impulse of the perturbation (Fig. 6A), $r = 0.96$ on average, in
275 spite of the slight differences observed in average peak force levels. Conversely,
276 the mean correlation between ΔCoP and force amplitude was poor ($r = 0.49$) and
277 not statistically significant in 7 out of 14 subjects (Fig. 6B). The box plots of Fig.
278 6C show the distribution of the individual Pearson's correlation coefficients in the
279 two cases.

280 The linearity of the relation between ΔCoP and impulse allowed normalizing the
281 CoP displacement to the impulse of the perturbation: $\Delta\text{CoP}_n = \frac{\Delta\text{CoP}}{\text{Impulse}}$, which
282 should then provide a postural index independent of the magnitude of perturbation
283 (Dvir et al. 2020). This index remained fairly constant, within the constant-force
284 series for impulse (range: 4-10 Ns). Friedman's ANOVA indicated a significant
285 dependence of ΔCoP_n with impulse ($p < 0.01$) with a significantly increased value
286 at impulse = 2 Ns compared to the other magnitudes ($p < 0.01$) (Fig. 7A). Also in
287 the constant-impulse session, the experimental ΔCoP_n was influenced by the force
288 amplitude of the perturbation ($p < 0.01$) but only the response to $F=100$ N differed
289 significantly from the other magnitudes (Fig. 7B): the ΔCoP_n at 100 N was
290 significantly higher than the ΔCoP_n at 20 N ($p < 0.05$) and at 40 N ($p < 0.01$).
291 Notably, on exclusion of the low-impulse (2 Ns) and high-force perturbations (100
292 N) the individual ΔCoP_n values remain fairly comparable, even in response to
293 different stimulus types (ICC = 0.88 with 95% confident interval [0.75 – 0.96]).
294 Furthermore, the normalized index ΔCoP_n showed relatively low variability when
295 assessed in response to 5 perturbations of the same type: on average $\text{CoV} = 13 \pm 7\%$.

296 A single index value was calculated for each subject by averaging the ΔCoP_n over
297 all perturbations greater than 2 Ns and less than 100 N (mean [range]: 0.93 [0.72 –
298 1.15] cm/Ns). The mean value of the ΔCoP_n was significantly inversely correlated
299 with the physical characteristics of the subjects: weight ($r = -0.79$), height ($r = -$
300 0.69) and foot length ($r = -0.63$).

301 In order to exclude postural adjustments in preparation for back perturbations, the
302 resting CoP was analyzed for possible variations during the test. No significant
303 change in resting CoP was detected within any of the 2 session and of the 8
304 perturbation sequences.

305 *3.2 Simulations results*

306 The tuning of the model was performed to match the average experimental ΔCoP_n
307 response of Fig. 7A (black line). The comparison between simulation results and
308 experimental data, for each testing condition selected during the trials carried out
309 on healthy subjects, is shown in Fig. 8.

310 It can be observed that, in the absence of sensory noise, simulated ΔCoP exhibited
311 a linear trend with the impulse (Fig. 8A, blue line) whereas no dependence on the
312 force amplitude (Fig. 8B) was found. Accordingly, ΔCoP_n remained extremely
313 constant over the entire range of impulse and force amplitude (Fig. 8C and D).

314 With the addition of noise to the sensory feedback, both ΔCoP and ΔCoP_n increased
315 in all conditions (Fig 8 A-D, red lines). While this effect was uniform for ΔCoP in
316 all conditions, it was particularly marked at low impulse for ΔCoP_n , thus faithfully
317 matching the experimental data at 2 Ns.

318 **4. DISCUSSION**

319 To the best of our knowledge, this is the first study in which force and impulse of
320 the trunk perturbations have been systematically varied in order to investigate their
321 differential effect on PR. The issue was addressed by challenging the balance of
322 healthy subjects by means of a custom-built perturbator, which proved adequate to
323 deliver accurately controlled stimuli, and by analyzing simulated responses based
324 on a simple inverse pendulum model.

325 The findings support the hypothesis formulated on the basis of a previous
326 observation, namely, that the displacement of the CoP is consistently and strongly
327 correlated with impulse and not significantly correlated with the force amplitude of
328 the perturbation. Furthermore, since the extracted ΔCoP_n was quite constant across
329 the perturbation range, the applicability of this index as a synthetic descriptor of the
330 individual postural performance was further amplified.

331 Although, as pointed out, the association between ΔCoP and the magnitude of the
332 perturbation has been highlighted before, a clear *linear* relationship has been
333 evidenced experimentally only in a handful of studies. Kim et al (2009) showed that
334 ΔCoP was positively correlated with the peak force of perturbations applied to the
335 high back, in apparent contrast with the present results. However, we speculate that
336 the duration of the perturbations (which was not measured) was quite constant
337 across the different subjects, which would make impulse and force amplitude
338 proportionally related and thus, both correlated with ΔCoP . Our preliminary study
339 on PR (Dvir et al. 2020) indicated a moderate correlation between ΔCoP and force
340 ($r = 0.50$) and a stronger correlation with the impulse of the perturbation ($r = 0.71$)

341 but the distributions of the individual Pearson correlation coefficients were quite
342 dispersed, possibly because the study was based on uncontrolled manually-
343 delivered perturbations. The possibility to deliver accurate perturbations in the
344 present study effectively reduced the intra-subject variability in the PR and revealed
345 the clear-cut linear relationship between ΔCoP and impulse ($r = 0.96$) while
346 confirming a low correlation between ΔCoP and force amplitude ($r = 0.49$ on
347 average but reaching significance only in 7 subjects). Moreover, the reproducibility
348 of the disturbances provided by the perturbator was adequate for the application, as
349 signaled by the results shown in Fig. 5, confirming that the performance of the
350 device was not significantly affected by the presence of a human operator (Ferraresi
351 et al. 2020b; Maffiodo et al. 2020). Notably, as compared to our previous study
352 based on manual uncontrolled perturbations, with the new perturbator we were able
353 to reduce the within-subject variability of ΔCoP_n , from about $20 \pm 8 \%$ (recalculated
354 from previous data) to $13 \pm 7 \%$. As a result, it was here possible to achieve a
355 comparable ICC with as few as 5 perturbations, instead of the 20 stimuli used in the
356 previous study.

357 The results of the study reinforce the concept that a single index, ΔCoP_n , obtained
358 from the ratio of ΔCoP and impulse, may synthetically describe the PR of the
359 subject, independently of the magnitude of the perturbation (Dvir et al. 2020). In
360 fact, this index is here shown to remain fairly constant in a wide range of force and
361 impulse intensity (Fig. 7). Notably, this index was slightly but significantly
362 increased at low impulse and high force amplitude: a pattern not predicted by the
363 model (Fig. 8 D). While significant non-linearities are embedded in the postural
364 control system, starting from the muscle level (Ivanenko and Gurfinkel 2018), the

365 present deviation from linearity could be related to the short duration of the
366 perturbation, which is below 75 ms for both 2 Ns and 100 N. In fact it has been
367 proposed that short stimuli elicit a triggered response, uninfluenced by the stimulus
368 characteristics, while a longer stimulus duration would be necessary for sensory
369 inputs to encode the magnitude of the perturbation and help to shape a proportionate
370 response (Diener et al. 1988). On the other hand, the results here obtained with the
371 model also suggest that, at low perturbation magnitudes, the presence of noise in
372 the system may account for a similar non-linearity (Fig 8 C-D).

373 While the implemented model completely excludes a dependence of the PR on the
374 force amplitude, a significant correlation was evidenced in some subjects (Fig. 6B).
375 It may be observed that these individual correlations are based on only 4 points and
376 thus heavily depend on each single measurement. As a consequence, increased
377 correlations would result due to the abnormally increased response at 100 N, as
378 previously discussed. On the other hand, a weak correlation with the force
379 amplitude could also result from the involvement of additional sensory feedback
380 pathways, particularly sensitive to the force stimulus (e.g., touch receptors of the
381 back, vestibular receptors), not included in the present model.

382 Regarding the accuracy of the simulations, the approach to model tuning used in
383 this study was considered suitable to achieve a realistic although simplified
384 behavior of the model, however it is well known that all the active and passive
385 response parameters discussed are highly subject-specific and require accurate
386 estimation when a detailed description of balance control is targeted (Goodworth
387 and Peterka 2018).

388 **5. LIMITATIONS**

389 As a first approximation, the balance reaction of healthy young adults in response
390 to low disturbance mainly consists of a correcting torque at the ankle (Horak and
391 Nashner 1986; Shumway-Cook and Woollacott 2007). Therefore, a single-link
392 inverted pendulum model was developed to simulate the postural response of the
393 study participants. This approximation was supported by the visual inspection of
394 the experimental trials, that confirmed how most oscillations occurred about the
395 ankle joints. As indicated by the good match between experimental and simulated
396 data, this simple model proved to be sufficiently accurate for the purpose of testing
397 the relationship between the displacement of the CoP and the impulse of the
398 perturbation. On the other hand, we cannot exclude that other postural strategies,
399 such as the hip strategy, could also contribute to the whole response, particularly to
400 high-magnitude perturbations. This would likely affect the correlation between
401 ΔCoP_n and impulse, although the precise effects are difficult to predict, based on
402 the present experiments. Appropriate integration of the hip strategy into the model
403 requires to adopt a double-link inverted pendulum model, resulting in a far more
404 complex optimization problem, with additional unknown control parameters used
405 to model the correcting torque at the hip and the interaction between active controls
406 at each joint (Goodworth and Peterka 2018). This, in turn, requires the acquisition
407 of additional descriptors of the postural response, e.g. tangential forces at the
408 platform, movements and acceleration of the different body segments. The present
409 results suggest that this increase in complexity is not necessary for describing the
410 response to small postural perturbation.

411 Another limitation of the study was the non-exactly constant value of the force
412 amplitude and of the impulse in the force constant session and in the impulse
413 constant session, respectively. The perturbations were applied to the subjects with
414 a custom-made device consisting of a low friction pneumatic actuator controlled in
415 force and position by a PI controller. The nonlinearities and relatively slow
416 dynamics associated to pneumatic systems and the inertia of the piston make the PI
417 controller not able to appropriately minimize the error between the force reference
418 profile and the applied force in a very short time. As a result, there is an overshoot
419 in the first 35 ms of the perturbation that impacts on the calculated Force Amplitude,
420 especially in the case of short-lasting perturbations. To obtain more accurate
421 perturbation profiles and more robust control, an electrically-actuated perturbator
422 based on Model Predictive Control, with inherent high dynamics and stiffness, is
423 currently under development (Pacheco Quiñones et al. 2021).

424 **6. CONCLUSION**

425 The results support the use of the impulse rather than the force as input variable in
426 impulsive perturbations applied to the trunk. Thanks to the linearity of the
427 relationship between ΔCoP and impulse, the postural index, ΔCoP_n , may be used
428 as a synthetic descriptor of the individual postural performance.

429 **CONFLICT OF INTEREST STATEMENT**

430 The authors have no conflict to disclose.

431 **ACKNOWLEDGMENTS**

432 This work was supported by grants from “Fondo Europeo di sviluppo regionale –
433 Regione Liguria” (ROAS_RIC_COMP_17_01) and by “Proof of Concept” Project
434 2018, the Politecnico di Torino. Funding sources had no role in the conduction of
435 the study.

436 **REFERENCES**

- 437 Azzi NM, Coelho DB, Teixeira LA (2017) Automatic postural responses are
438 generated according to feet orientation and perturbation magnitude. *Gait*
439 *Posture* 57:172–176. doi: 10.1016/j.gaitpost.2017.06.003
- 440 Boonstra TA, Schouten AC, Van Der Kooij H (2013) Identification of the
441 contribution of the ankle and hip joints to multi-segmental balance control. *J*
442 *Neuroeng Rehabil* 10:23. doi: 10.1109/TNSRE.2014.2372172
- 443 Bortolami SB, DiZio P, Rabin E, Lackner JR (2003) Analysis of human postural
444 responses to recoverable falls. *Exp Brain Res* 151:387–404. doi:
445 10.1007/s00221-003-1481-x
- 446 Chen B, Lee YJ, Aruin AS (2017) Role of point of application of perturbation in
447 control of vertical posture. *Exp Brain Res* 235:3449–3457. doi:
448 10.1007/s00221-017-5069-2
- 449 Colebatch JG, Govender S (2019) Responses to anterior and posterior
450 perturbations in Parkinson’s disease with early postural instability: role of
451 axial and limb rigidity. *Exp Brain Res* 237:1853–1867. doi:
452 <https://doi.org/10.1007/s00221-019-05553-8>
- 453 Colebatch JG, Govender S, Dennis DL (2016) Postural responses to anterior and
454 posterior perturbations applied to the upper trunk of standing human
455 subjects. *Exp Brain Res* 234:367–376. doi: 10.1007/s00221-015-4442-2
- 456 Diener HC, Horak FB, Nashner LM (1988) Influence of stimulus parameters on

457 human postural responses. *J Neurophysiol* 59:1888–1905. doi:
458 10.1152/jn.1988.59.6.1888

459 Dvir Z, Paterna M, Quargnenti M, et al (2020) Linearity and repeatability of
460 postural responses in relation to peak force and impulse of manually
461 delivered perturbations : a preliminary study. *Eur J Appl Physiol* 120:1319–
462 1330. doi: 10.1007/s00421-020-04364-y

463 Engelhart D, Schouten AC, Aarts RGKM, Van Der Kooij H (2015) Assessment of
464 Multi-Joint Coordination and Adaptation in Standing Balance : A Novel
465 Device and System Identification Technique. *IEEE Trans Neural Syst*
466 *Rehabil Eng* 23:973–982. doi: 10.1109/TNSRE.2014.2372172

467 Ferraresi C, De Benedictis C, Muscolo GG, et al (2020a) Development of an
468 Automatic Perturbator for Dynamic Posturographic Analysis. *Mechanisms*
469 *ans Machine Science* 93:273–282. doi: 10.1007/978-3-030-58104-6

470 Ferraresi C, Maffiodo D, Franco W, et al (2020b) Hardware-In-the-Loop
471 Equipment for the Development of an Automatic Perturbator for Clinical
472 Evaluation of Human Balance Control. *Appl Sci* 10:8886. doi:
473 10.3390/app10248886

474 Forghani A, Preuss R, Milner TE (2017) Effects of amplitude and predictability of
475 perturbations to the arm on anticipatory and reactionary muscle responses to
476 maintain balance. *J Electromyogr Kinesiol* 35:30–39. doi:
477 <http://dx.doi.org/10.1016/j.jelekin.2017.05.006>

478 Fujimoto M, Bair WN, Rogers MW (2015) Center of pressure control for balance
479 maintenance during lateral waist-pull perturbations in older adults. *J*
480 *Biomech* 48:963–968. doi: 10.1016/j.jbiomech.2015.02.012

481 Goodworth AD, Peterka RJ (2018) Identifying mechanisms of stance control : A
482 single stimulus multiple output model-fit approach. *J Neurosci Methods*
483 296:44–56. doi: 10.1016/j.jneumeth.2017.12.015

484 Grassi L, Rossi S, Studer V, et al (2017) Quantification of postural stability in
485 minimally disabled multiple sclerosis patients by means of dynamic
486 posturography: An observational study. *J Neuroeng Rehabil* 14:4. doi:
487 10.1186/s12984-016-0216-8

488 Horak FB, Nashner LM (1986) Central programming of postural movements:
489 adaptation to altered support-surface configurations. *J Neurophysiol*
490 55:1369–81. doi: 10.1152/jn.1986.55.6.1369

491 Ivanenko Y, Gurfinkel VS (2018) Human postural control. *Front Neurosci*
492 12:171. doi: 10.3389/fnins.2018.00171

493 Kim J, Kim C, Lee J, et al (2009) Human postural control against external force
494 perturbation applied to the high-back. *Int J Precis Eng Manuf* 10:147–151.
495 doi: 10.1007/s12541-009-0083-3

496 Kim S, Atkeson CG, Park S (2012) Perturbation-dependent selection of postural
497 feedback gain and its scaling. *J Biomech* 45:1379–1386. doi:
498 10.1016/j.jbiomech.2012.03.001

499 Maaswinkel E, Griffioen M, Perez RSGM, van Dieën JH (2016) Methods for
500 assessment of trunk stabilization, A systematic review. *J Electromyogr*
501 *Kinesiol* 26:18–35. doi: 10.1016/j.jelekin.2015.12.010

502 Maffiodo D, Franco W, De Benedictis C, et al (2020) Pneumo-tronic Perturbator
503 for the Study of Human Postural Responses. *Advances in Intelligent Systems*
504 *and Computing* 980:374–383. doi: 10.1007/978-3-030-19648-6_43

505 Martinelli AR, Coelho DB, Magalhães FH, et al (2015) Light touch modulates
506 balance recovery following perturbation: from fast response to stance
507 restabilization. *Exp Brain Res* 233:1399–1408. doi: 10.1007/s00221-015-
508 4214-z

509 Morasso PG, Baratto L, Capra R, Spada G (1999) Internal models in the control
510 of posture. *Neural Networks* 12:1173–1180. doi: 10.1016/S0893-
511 6080(99)00058-1

512 Pacheco Quiñones D, Paterna M, De Benedictis C (2021) Automatic
513 electromechanical perturbator for postural control analysis based on model
514 predictive control. *Appl Sci* 11:4090. doi: 10.3390/app11094090

515 Pasma EP, McKeown MJ, Cleworth TW, et al (2019) A novel MRI compatible
516 balance simulator to detect postural instability in parkinson’s disease. *Front*
517 *Neurol* 10:922. doi: 10.3389/fneur.2019.00922

518 Pidcoe PE, Rogers MW (1998) A closed-loop stepper motor waist-pull system for
519 inducing protective stepping in humans. *J Biomech* 31:377–381. doi:

- 520 10.1016/S0021-9290(98)00017-7
- 521 Robbins SM, Caplan RM, Aponte DI, St-Onge N (2017) Test-retest reliability of a
522 balance testing protocol with external perturbations in young healthy adults.
523 *Gait Posture* 58:433–439. doi: 10.1016/j.gaitpost.2017.09.007
- 524 Robert T, Vallee P, Tisserand R (2018) Stepping boundary of external force-
525 controlled perturbations of varying durations : Comparison of experimental
526 data and model simulations. *J Biomech* 75:89–95. doi:
527 10.1016/j.jbiomech.2018.05.010
- 528 Schmidt D, Germano AMC, Milani TL (2015) Aspects of dynamic balance
529 responses: Inter- and intra-day reliability. *PLoS One* 10:e0136551. doi:
530 <http://dx.doi.org/10.1371/journal.pone.0136551>
- 531 Shumway-Cook A, Woollacott MH (2007) *Motor Control: Translating research*
532 *into clinical practice*, 3rd edn. Lippincott Williams & Wilkins, Philadelphia,
533 Pa, USA.
- 534 Sturnieks DL, Menant J, Delbaere K, et al (2013) Force-Controlled Balance
535 Perturbations Associated with Falls in Older People: A Prospective Cohort
536 Study. *PLoS One* 8:e70981. doi: 10.1371/journal.pone.0070981
- 537 Teixeira LA, Azzi N, de Oliveira JÁ, et al (2019) Automatic postural responses
538 are scaled from the association between online feedback and feedforward
539 control. *Eur J Neurosci* 1–10. doi: 10.1111/ejn.14625
- 540 Van Der Kooij H, Peterka RJ (2011) Non-linear stimulus-response behavior of the

541 human stance control system is predicted by optimization of a system with
542 sensory and motor noise. *J Comput Neurosci* 30:759–778. doi:
543 10.1007/s10827-010-0291-y

544 Van Der Kooij H, Van Asseldonk E, Van Der Helm FCT (2005) Comparison of
545 different methods to identify and quantify balance control. *J Neurosci*
546 *Methods* 145:175–203. doi: 10.1016/j.jneumeth.2005.01.003

547 Winter DA, Patla AE, Prince F, et al (1998) Stiffness control of balance in quiet
548 standing. *J Neurophysiol* 80:1211–1221. doi: 10.1152/jn.1998.80.3.1211

549

550

551 **FIGURE LEGENDS**

552 **Figure 1.** Experimental Set-up. A: pneumo-tronic perturbator, 1: low friction
553 pneumatic actuator, 2: flow-proportional valves, 3: laser sensor, 4: load cell,
554 5: end striker, 6: handles, 7: trigger button. B: Example of experimental task
555 with the operator handling the pneumo-tronic perturbator.

556 **Figure 2.** Force profiles for the different perturbation types included in the constant
557 force series (A) and the constant impulse series (B). The intended force
558 profile (red) is superimposed to the actually delivered force profile (blue,
559 average across all subjects).

560 **Figure 3.** A representative recording of the perturbation (Black line) and the
561 ensuing displacement of the Center of Pressure (dashed grey line) observed

562 during experimentation (constant-force series: 40 N, 6 Ns).

563 **Figure 4.** Free body diagram of a single-link inverted pendulum model for postural
564 control analysis. θ is the body oscillation, l is the height of the subject with
565 respect to the ankle joint; h_F is the distance between ankle joint and the point
566 of application of the perturbation force F_e ; d is the distance between ankle
567 joint and the center of mass (CoM); h is the height of ankle joint with respect
568 to the fixed base of support; I is the rotational inertia of the body about the
569 CoM; m is the subject body mass; \ddot{x} is the horizontal acceleration of the CoM;
570 \ddot{y} is the vertical acceleration of the CoM; $\ddot{\theta}$ is the angular acceleration of the
571 CoM; g is the gravitational acceleration; τ is the correcting torque at the
572 ankle; CoP is the center of pressure position; R_x is the horizontal component
573 of the ground reaction force; R_y is the vertical component of the ground
574 reaction force

575 **Figure 5.** Characteristics of delivered perturbations for the constant-force series
576 (left) and the constant-impulse series (right). Each box represents the median
577 and the standard deviation of the perturbations applied to the subjects (n=5
578 perturbation x 14 subjects = 70), for each stimulus type.

579 **Figure 6.** The relationship between the maximum displacement of the center of foot
580 pressure, ΔCoP , and the magnitude of the perturbations, in terms of impulse
581 (A) and force amplitude (B) for each participant in the experimental trial.
582 Distribution of the Pearson's Correlation Coefficients, for the ΔCoP –
583 Impulse (Black) and the ΔCoP - Force (white) correlation (C).

584 **Figure 7.** The relationship between the postural index ΔCoP_n and the magnitude of
585 perturbation expressed in terms of impulse (A) and force amplitude (B) for
586 each participant in the experimental trial (colored line). The thick black line
587 represents the average trend.

588 **Figure 8** The relationship between the simulated maximum displacement of the
589 center of foot pressure, ΔCoP , and the magnitude of the perturbations, in
590 terms of impulse (A) and force amplitude (B). The relationship between the
591 postural index ΔCoP_n and the magnitude of perturbation expressed in terms
592 of impulse (C) and force amplitude (D).

593 Red lines refer to the results of the simulation performed considering the
594 sensorial noise; blue lines refer to the results of the simulation performed
595 without the contribution of the sensorial noise; black lines are the average
596 experimental trend calculated on all the participants of the experimental
597 analyses.

598

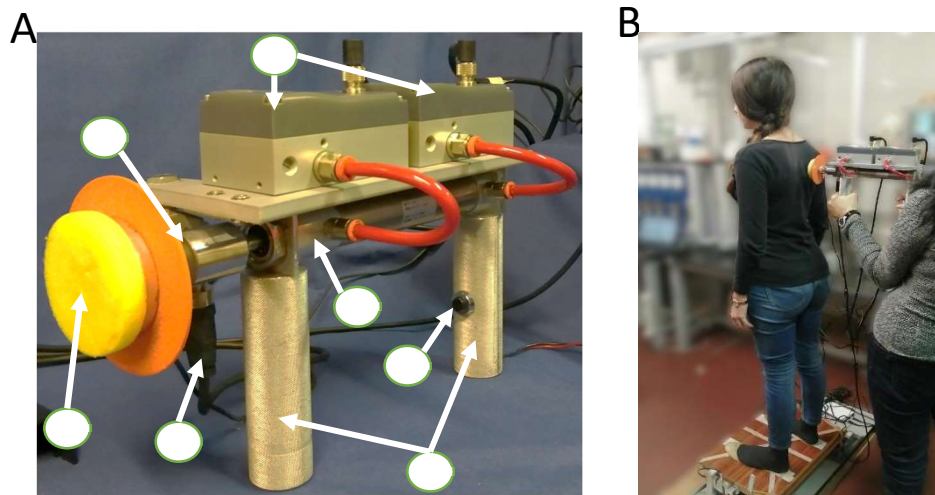


Figure 1

600

601

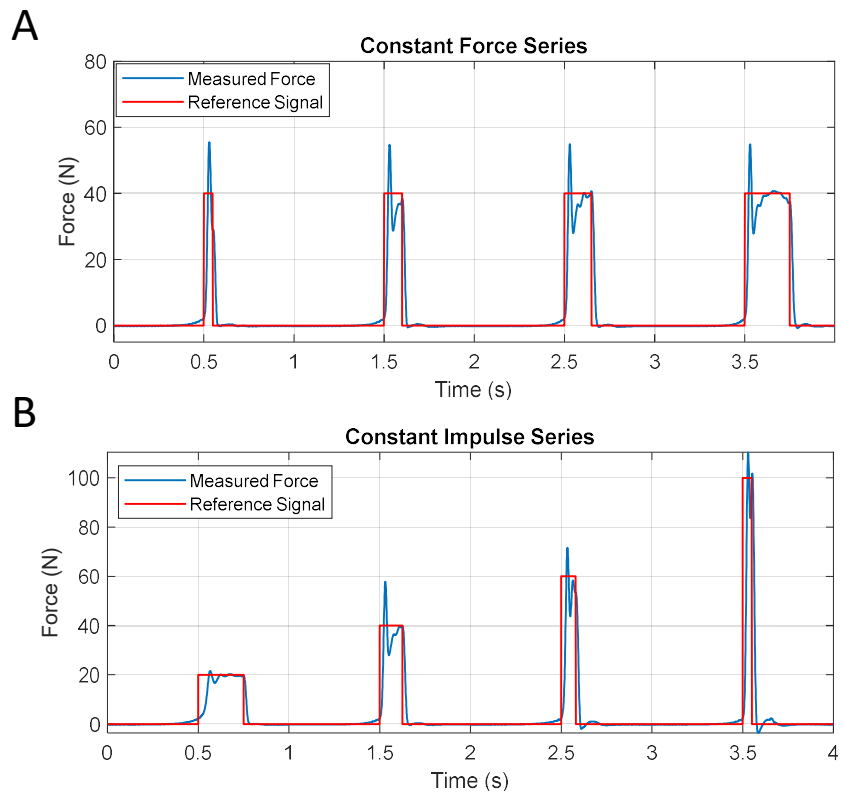
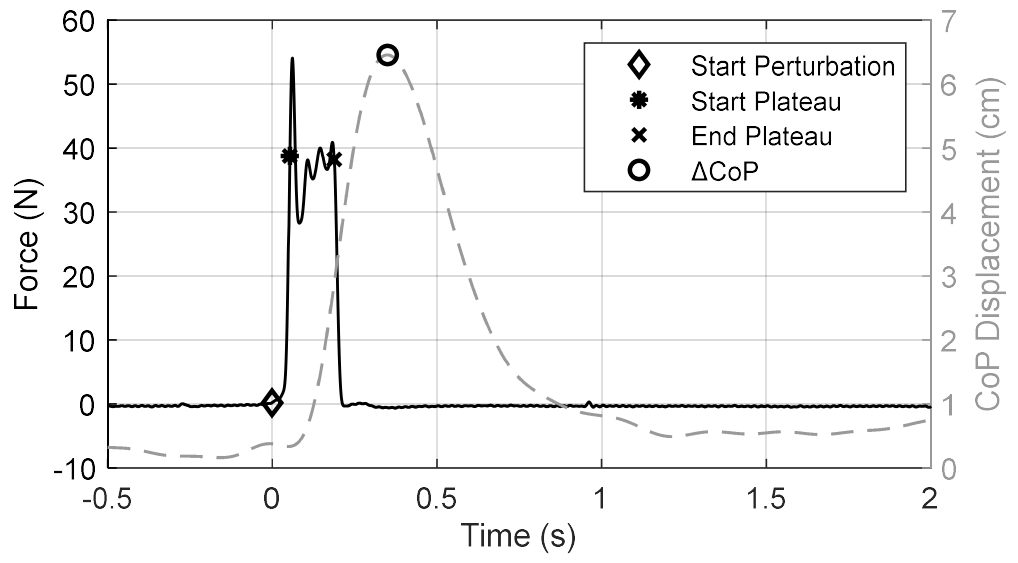


Figure 2

**Figure 3**

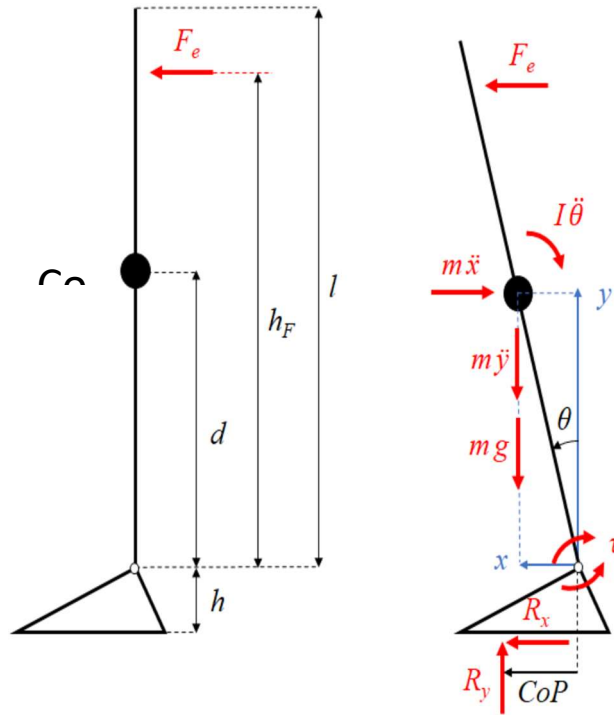
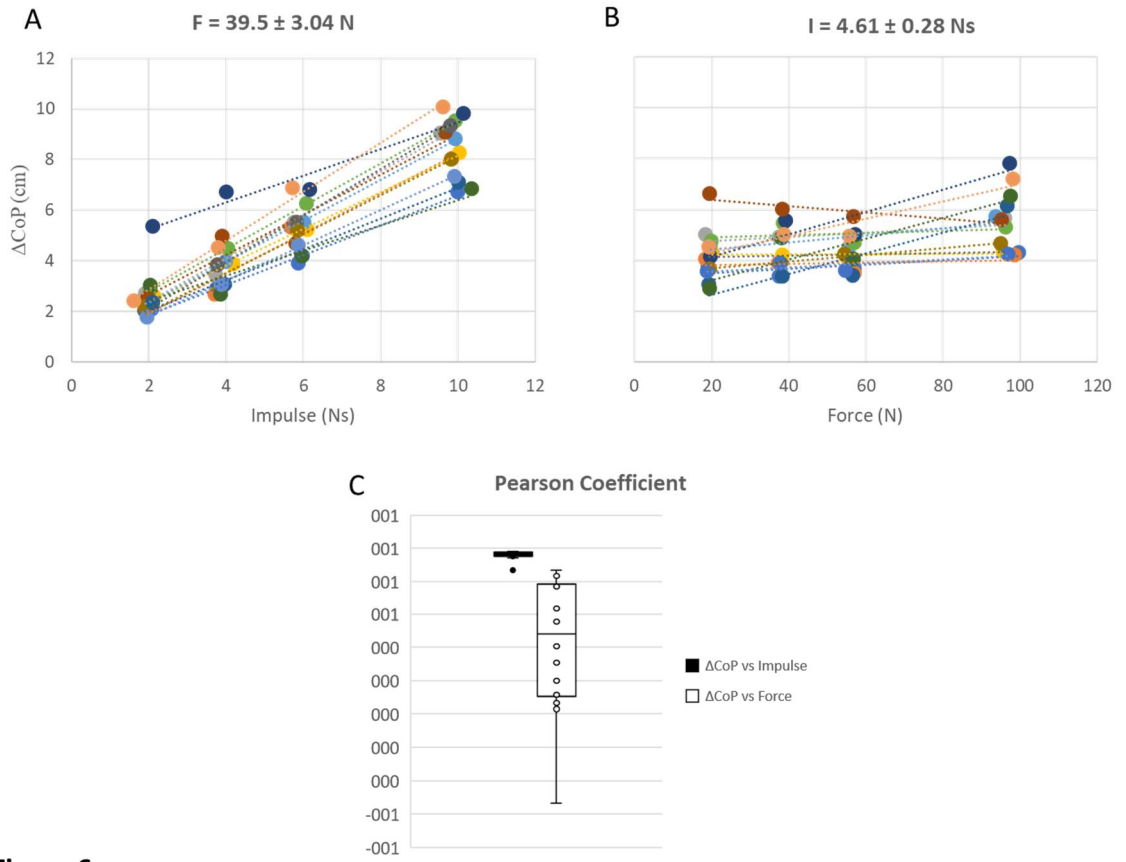
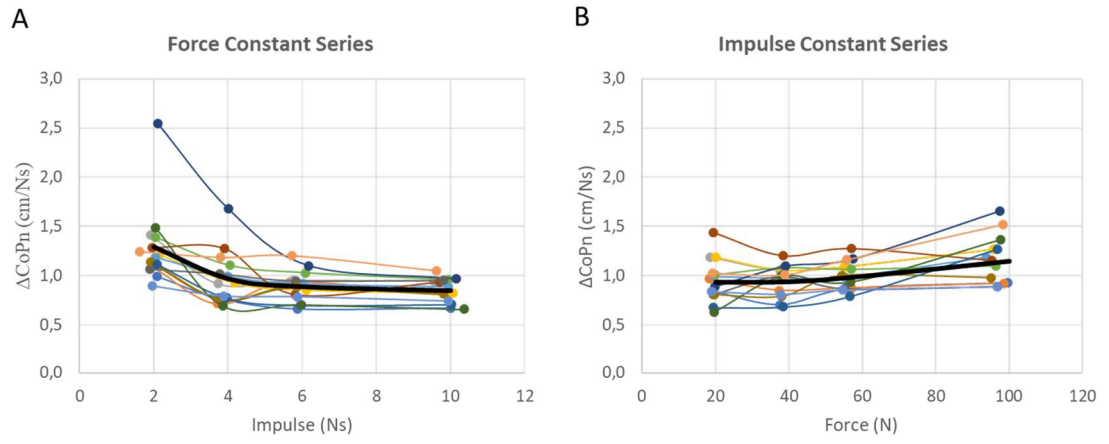


Figure 4



604 **Figure 6**



605 **Figure 7**

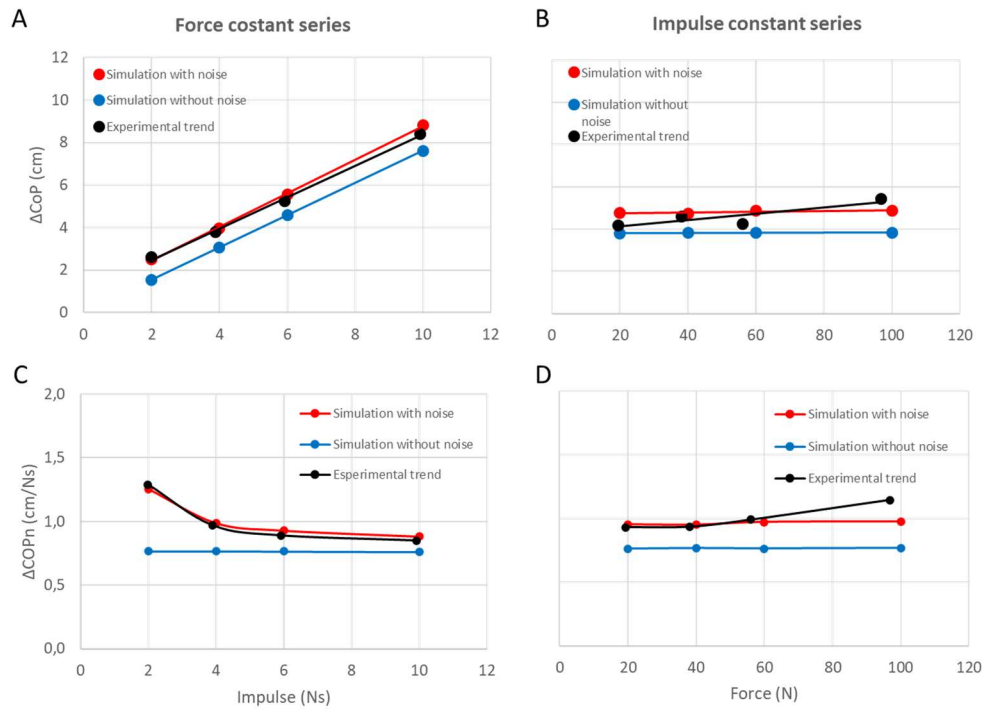


Figure 8

606